UPDATED GOODMAN DIAGRAMS FOR FIBERGLASS

COMPOSITE MATERIALS

USING THE DOE/MSU FATIGUE DATABASE

by

Herbert J. Sutherland
Sandia National Laboratories[1]
Albuquerque, NM 87185-0708
hjsuthe@sandia.gov

and

John F. Mandell
Montana State University
Bozeman, MT 59717
johnm@coe.montana.edu

Abstract

Recent expansions of the DOE/MSU Composite Fatigue Database permit the construction of a high resolution Goodman Diagram with detailed information at thirteen R-values (minimum stress / maximum stress). This Goodman diagram is the most detailed to date, including several loading conditions which have been poorly represented in earlier studies. The data for a single E-glass/polyester material system are extracted from the MSU/DOE Fatigue Database to construct the Goodman diagrams. Diagrams are constructed using both mean fits to the data and 95/95 fits. These formulations allow the effects of mean stress on damage calculations to be evaluated. Two sets of load spectra are analyzed. The first set is experimentally-determined load spectra obtained from operating wind turbines, and the second is the WISPERX load spectrum. The analysis of the turbine load spectra illustrates a significant overestimation of the equivalent fatigue loads when the mean stress is not considered in the calculation. The analysis of coupon data using the WISPERX spectrum illustrates that the Miner's rule does not predict failure very well.

---

[1] *Sandia is a multiprogram laboratory operated by Sandia Corporation, a Lockheed Martin company, for the U.S. Department of Energy under contract DE-AC04-94AL85000

Introduction

Most turbine blades are constructed from low cost forms of composite materials, with manufacturing primarily by wet hand lay-up or resin infusion using woven or stitched E-glass fabric architectures. Some blades also use relatively low cost, low cure temperature forms of prepreg. While finished blade costs are on the order of $10/Kg, the performance required of blades is impressive, with higher levels of fatigue cycling than for most fixed wing or rotary aircraft blades [1]. As wind turbines expand in both size and importance, improvements in materials and lifetime prediction methodologies are essential. Reviews of blade loadings and material response may be found in References 1 through 4. References 1 through 3, as well as most of the remaining cited papers and the database are available through the Sandia National Laboratories website: http://www.sandia.gov/wind/.

The damage analysis of wind turbine blades requires a detailed description of the fatigue load spectra and the fatigue behavior of blade material. The latter is typically presented as a Goodman diagram in which the cycles-to-failure are plotted as a function of mean stress and range along lines of constant R-values [1]. The R-value for a fatigue cycle is defined as:

$$R = \frac{\sigma_{min}}{\sigma_{max}} \quad , \tag{1}$$

where σ_{min} is the minimum stress and σ_{max} is the maximum stress in a fatigue stress cycle (tension is considered positive and compression is negative).

As the Goodman diagram is a non-linear function for typical wind turbine blade materials, many analyses completely ignore the effects of mean stress on the determination of damage in composite wind turbine blades. Even when a "complete" Goodman diagram is used, available Goodman diagrams for the fiberglass composite materials typically used in wind turbine blades are relatively sparse with material characterization at only five or six R-values [1, 5 and 6].

In recent publications, Mandell et al [7 and 8] have presented a detailed Goodman diagram for these fiberglass materials. Their formulation uses the MSU/DOE Fatigue Database [2, 3] to develop a Goodman diagram with information at thirteen R-values. This diagram is the most detailed to date, and it includes several loading conditions that have been poorly represented in earlier studies. Both mean and 95/95 fits of the data are developed. These formulations allow the effects of mean stress on damage calculations to be evaluated with greater accuracy.

To illustrate the effect of the updated Goodman diagram on the fatigue analysis of wind turbine blades, two applications are presented. In the first, Sutherland and Mandell [9] analyze the load spectra from two operating wind turbines using Equivalent Fatigue Loads, EFL [1]. In the second application, Sutherland and Mandell [8] examine the failures of coupons subjected to the WISPERX spectrum [10].

Fatigue Data

The DOE/MSU fatigue database contains over 8800 test results for over 130 material systems. The database contains information on composite materials typically used in wind turbine applications that are constructed from fiberglass and carbon fibers in a variety of matrix materials. References 2, 3 and 11 provide a detailed analysis of data trends and blade substructure applications.

Recent efforts to improve the accuracy of spectrum loading lifetime predictions for fiberglass composites have led to the development of a more complete Goodman diagram than previously available, and a more accurate fatigue model.

Constant Amplitude Data

The material under consideration here is a typical fiberglass laminate that is called DD-16 in the DOE/MSU Database. This laminate has a $[90/0/\pm45/0]_S$ configuration with a fiber volume fraction of 0.36. The 90° and 0° plies are D155 stitched unidirectional fabric, the ±45° plies are DB120 stitched fabric, and the resin is an ortho-polyester. Mandell et al [2, 12] described the test methodologies used to obtain the data cited here. This material has a static tensile strength of 625 MPa and a compressive strength of 400 MPa. The 95/95 strength values are 510 MPa and 357 MPa, respectively. These strength values were determined at a strain rate similar to that of the fatigue tests.

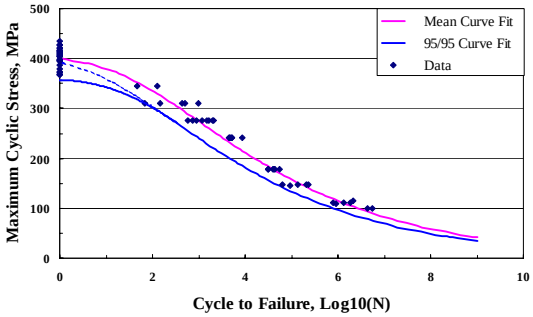

Figure 1a: Data for R= -1.

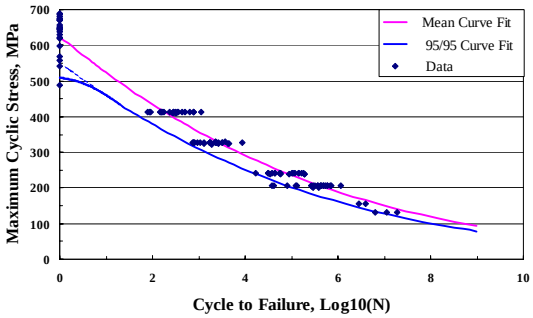

Figure 1b: Data for R=0.1

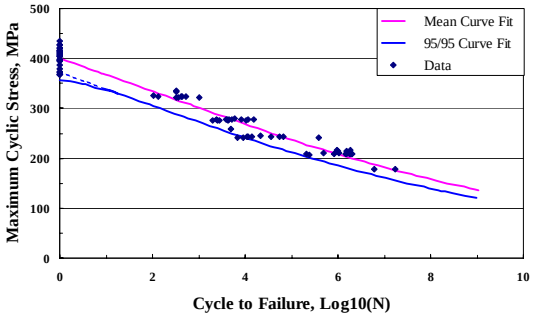

Figure 1c: Data for R= 10

Figure 1: Maximum Absolute Stress versus Cycles to Failure for Thirteen R-Values for Database Material DD16

For illustrative purposes, the constant amplitude data at R = -1, 0.1 and 10 are shown in Fig. 1. A complete set of the data for all thirteen R-values is available in Refs. 2 and 8.

Curve Fits

Mean Fit

As presented by Mandell et al [2], the constant amplitude data at 13 R-values were fit with a three-parameter equation of the following form:

$$\sigma_O - \sigma = a\sigma \left[\frac{\sigma}{\sigma_O}\right]^b (N^C - 1) \quad , \tag{2}$$

where σ is the maximum applied stress, σ_o is the ultimate tensile or compressive strength (obtained at a strain rate similar to the 10 Hz fatigue tests), and a, b, and c are the fitting parameters.

The results of these fits are summarized in Table I and in Fig. 1.

The parameters in these curve fits were selected to provide the best fit to the experimental data and to provide a 10^9 cycle extrapolation stress which was within ten (10) percent of the extrapolation from a simple two-parameter power law fit to the fatigue data having lifetimes greater than 1000 cycles. [2]

95/95 Fit

Sutherland and Mandell [8] used these data to construct the "95/95" Goodman diagram. The 95/95 implies that, with a 95 percent level of confidence, the material will meet or exceed this design value 95 percent of the time.

The number of cycles to failure for the 95/95 fit is given by:

$$\log_{10}[N_{95/95}] = \log_{10}[N] + \log_{10}[N_o] \quad , \tag{3}$$

where N is determined from Eq. 2 and $\log_{10}[N_o]$ is shown in Table I for each of the thirteen R-values.

As shown in Fig. 1, this technique works well for the fatigue data, but in many cases, it predicts a 95/95 static strength that is not in agreement with the calculated value (see the dotted line in the figure). To rectify this situation, the 95/95 fatigue curve was "faired" into the measure 95/95 static strength, as shown by the solid lines in the figure [13].

Table I: Parameters for the Thirteen R-Values for Material DD16 and for Small Strands

R-Value	Model (Eq. 2)			95/95 (Eq. 3)
	a	b	c	$\log_{10}(N_o)$
1.1	0.06	3	0.05	4.43
1.43	0.06	3	0.15	1.85
2	0.06	4	0.25	2.67
10	0.1	4	0.35	0.87
–2	0.01	4	0.55	0.59
–1	0.02	3	0.62	0.53
–0.5	0.45	0.85	0.25	0.64
0.1	0.42	0.58	0.18	0.70
0.5	0.075	2.5	0.43	0.79
0.7	0.04	2.5	0.45	0.65
0.8	0.035	2.5	0.4	0.79
0.9	0.06	2.5	0.28	1.20
1*	0.21	3	0.14	3.03

*Assumes a frequency of 10 Hz.

Goodman Diagrams

For the analysis of S-N data, the preferred characterization is the Goodman diagram. In this formulation, the cycles-to-failure are plotted as functions of mean stress and amplitude along lines of constant R-values. Between R-value lines, the constant cycles-to-failure plots are typically, but not always, taken to be straight lines.

Various Goodman diagrams for the DD-16 fiberglass composite are shown in Figs. 2 and 3. These figures are presented in increasing level of knowledge about the S-N behavior of the fiberglass composite material. Figures 2a and 3a illustrate the "linear" Goodman diagram. In these two figures, the diagrams are constructed using the static strength values for the tensile and compressive intercepts of the constant life curves with the horizontal axis of the diagram and the S-N data for the R = –1 (see Fig. 1a) for the intercepts of the vertical axis. The "bi-linear" Goodman diagrams, shown in Figs. 2b and 3b, are constructed by adding the R = 0.1 S-N data (see Fig. 1b) to the diagram. The "full" Goodman diagrams, shown in Figs. 2c and 3c, are constructed by adding the data for the remaining eleven R-values.

Mean and 95/95 Diagrams

The Goodman diagrams shown in Fig. 2 were constructed using Eq. 2 and the information in Table I. Figures 2a and 2b, use the mean static strengths for the intercepts of the constant-life curves with the mean stress (horizontal) axis. Fig. 2c departs from traditional formulations in that the intercept for tensile mean axis (R = 1) is not the mean static strength. Rather, the intercept is a range of values based upon time-to-failure under constant load. These data were converted to cycles by assuming a frequency of 10 cycles/second, typical of the cyclic tests. Nijssen et al [14] have hypothesized a similar formulation previously.

The Goodman diagrams cited in Fig. 3 were constructed using Eqs. 2 and 3, the information in Table I, and the fairing of the S-N curves into the 95/95 static strengths. Again, the tensile intercept in Fig. 3c is a range of values based upon time under load.

Comparison

The Goodman diagrams presented in Figs. 2 and 3 are compared with one another in Fig. 4. The significant differences in the Goodman formulations are highlighted in Fig. 4. The area near the R = –1 axis is very important. This is the region where the fiberglass composite is in transition between compressive and tensile failure modes and many of the stress cycles on a wind turbine blade have an R-value near –1. The effect of the mode change on fatigue properties is illustrated by the direct comparison of the constant life curves for the three Goodman diagrams. In Fig. 4, the constant life curves for the three formulations of the Goodman diagram at 10^5 cycles are compared to one another.

Four distinct regions of comparison are noted: (1) the region of relatively high compressive mean stress ($1< R < \infty$, i.e., essentially the region to the left of R = 10); (2) the region of relatively low compressive stress ($-\infty < R < -1$; i.e., essentially the region between R = 10 and R = 1); (3) the region of relatively low tensile stress ($-1 < R < 0$; i.e., essentially the region between R = –1 and R = 0.1); and (4) the region of relatively high tensile stress ($1 < R < 0$; i.e.,

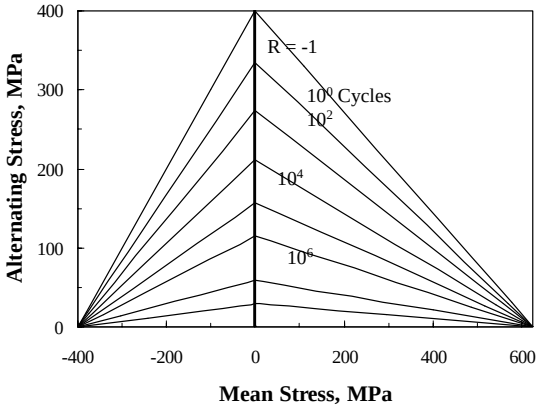

Fig. 2a: Linear Goodman Diagram

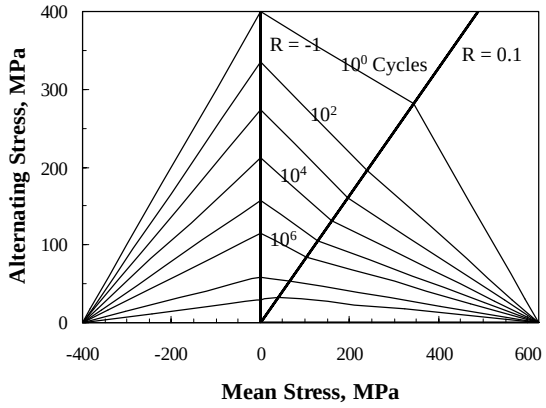

Fig. 2b: Bi-Linear Goodman Diagram

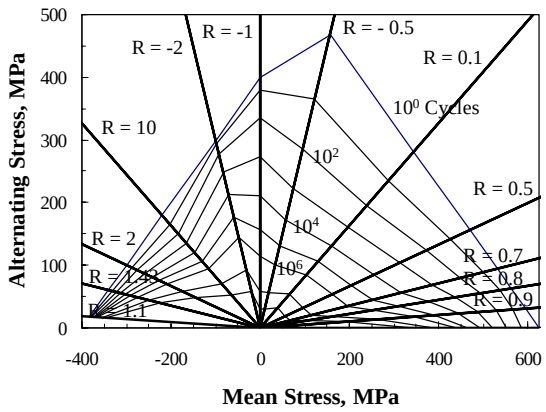

Fig. 2c: Full Goodman Diagram with Thirteen R-Values

Fig. 2. Mean Goodman Diagrams for Database Material DD16, Fit with Eq. 2

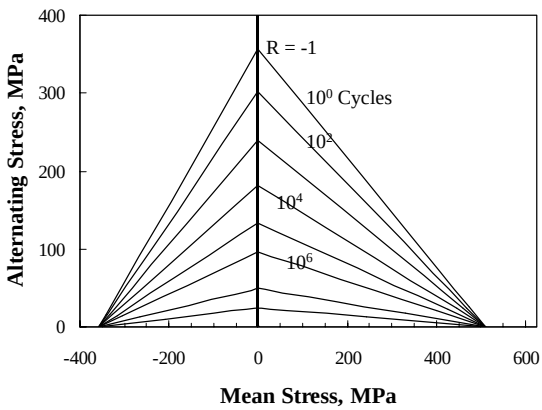

Fig. 3a: Linear Goodman Diagram

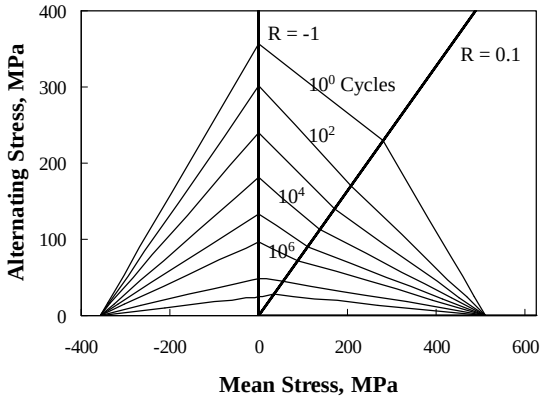

Fig. 3b: Bi-Linear Goodman Diagram

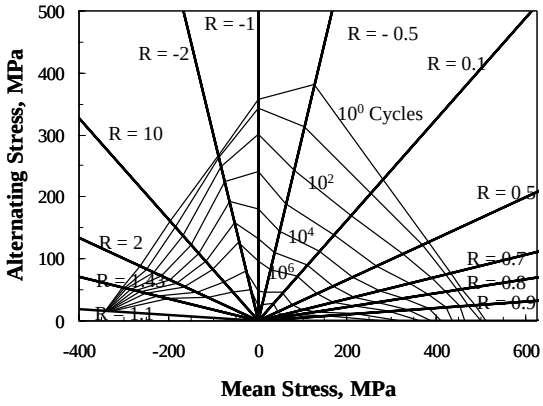

Fig. 3c: Full Goodman Diagram with Thirteen R-Values

Fig. 3. 95/95 Goodman Diagrams for Database Material DD16, Fit with Eqs. 2 and 3

essentially the region to the right of R = 0.1). In the first and third regions, the three formulations lie close to one another. Thus, each of the three formulations will predict approximately the same damage rate for the stress cycles in this range. For the fourth region (high tensile stress) the database formulation is below the linear and bi-linear formulations. Thus, the database formulation is more severe (i.e., it produces a shorter predicted service lifetime) than the other two. And, finally, for the second region (low compressive stress), the database formulation is above the linear and bi-linear formulations. Thus, it is less severe. Regions 2 and 3 are where the composite is in transition between compressive and tensile failure modes.

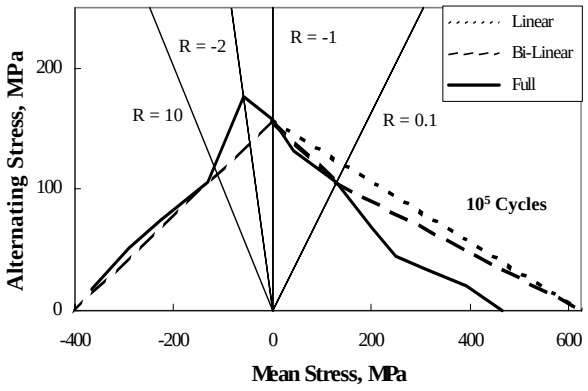

Fig. 4: Comparison of the Three Goodman Diagrams at 10^5 Cycles

Analysis of Load Spectra

To evaluate the effects of the improved Goodman diagram on damage calculations requires a detailed knowledge of the load (and stress or strain) spectra. For this analysis we will examine both experimental and test load spectra. Sutherland and Mandell [8, 9] originally conducted the analysis of these spectra.

Experimental Load Spectra

The LIST (Long-term Inflow and Structural Test) program has obtained long-term load spectra for two turbines. The first is a three-bladed Micon 65/13M wind turbine[15-17]. This turbine is being tested at a USDA site located near Bushland, Texas. This site is representative of most Great Plains commercial sites [18, 19]. The second turbine is the ART (Advanced Research Turbine). This Westinghouse 600-kW wind turbine is currently located at the National Wind Technology Center (NWTC) near Boulder, Colorado. Typical load spectra from these turbines are shown in Figs. 5 and 6.

WISPER Load Spectra

Wahl et al [12] have conducted spectral loading tests of coupons using the WISPERX spectrum [10]. The WISPERX spectrum is the WISPER spectrum with the small amplitude fatigue cycles removed. The remaining spectrum, see Fig. 7, consists of over 25,000 peaks-and-valleys (load reversal points). The original formulation of the spectrum is in terms of load levels that vary from 0 to 64 with zero at load level 25. For testing, the load levels were changed to the normalized form shown in the figure. In this form, the load at each reversal is ratioed to the maximum load. Thus, the test spectrum is a simple multiple of these reversal points by the maximum load in the spectrum. In this form, the maximum load in the spectrum is 1.0 and the minimum is –0.6923.

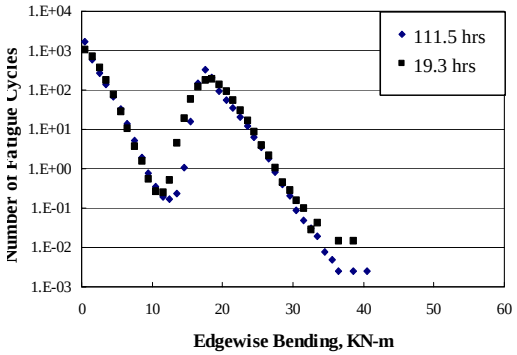

Fig. 5a: Edge-Bending in the Root of Blade 1

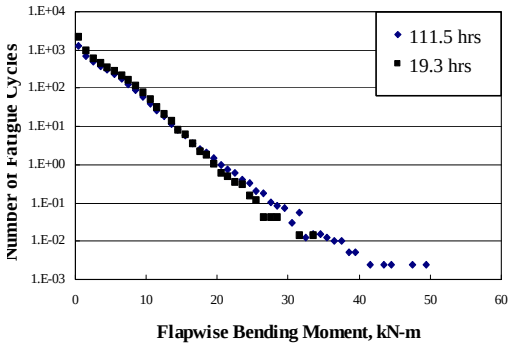

Fig. 5b: Flap-Bending in the Root of Blade 1

Fig. 5: Fatigue Load Spectrum for the 11-13 m/s Wind Speed bin for the Bushland Turbine

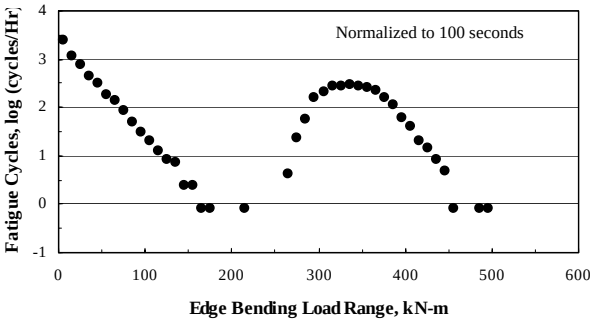

Fig. 6a: Edgewise Bending Moment

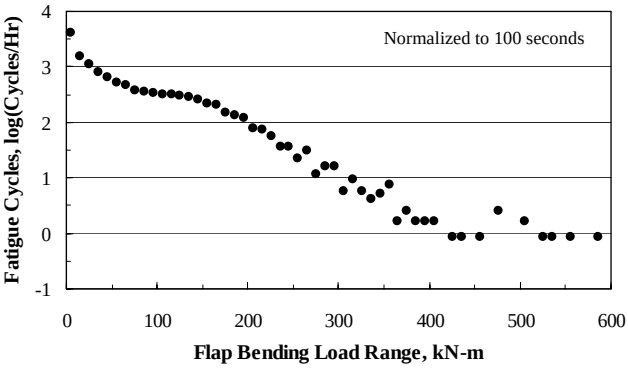

Fig. 6b: Flatwise Bending Moment

Fig. 6: Typical Fatigue Spectra for Root Bending Moments, >17 m/s Wind Speed Bin for the ART

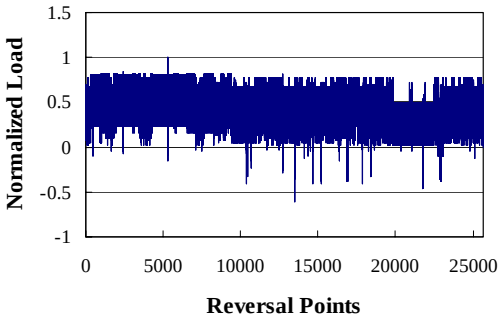

Fig. 7: Normalized WISPERX Spectrum

Results and Discussion

Experimental Load Spectra

The LIST data from both the Bushland turbine and the ART are analyzed using the Goodman diagrams shown in Figs. 2 and 3. The three Goodman diagrams are used to convert the load spectra, at various mean wind speed bins, to equivalent fatigue loads (EFLs) [1, 9]. For comparison purposes, the EFL using a constant fatigue exponent of 10 and a reference cycle count of 2000 cycles. This value of the fatigue exponent is typical of fiberglass composite materials.

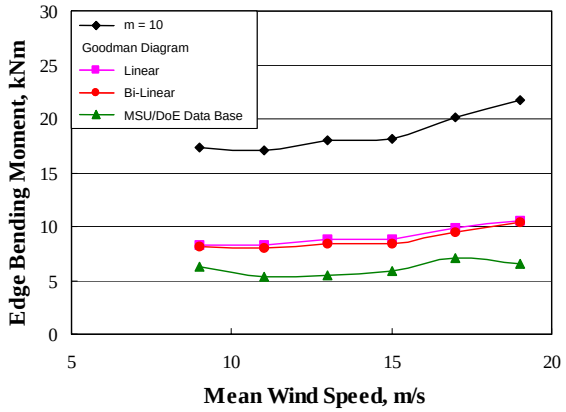

Fig. 8a: Edgewise Bending Moment

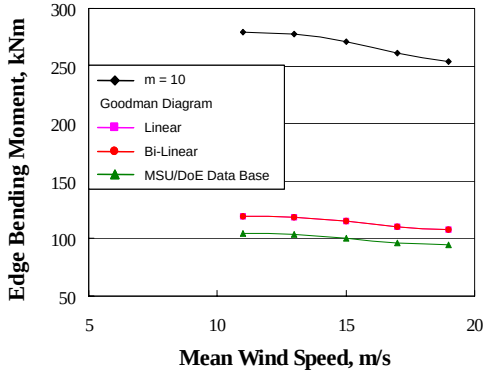

Fig. 9a: Edgewise Bending Moment

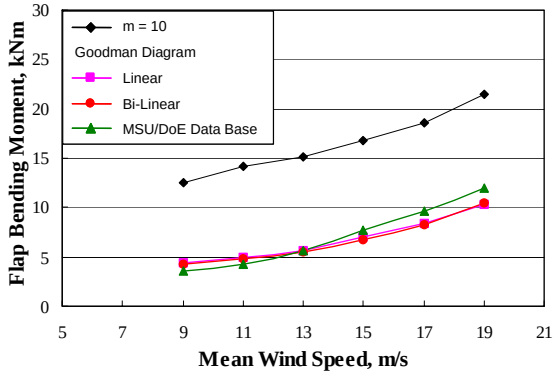

Fig. 8b: Flapwise Bending Moment

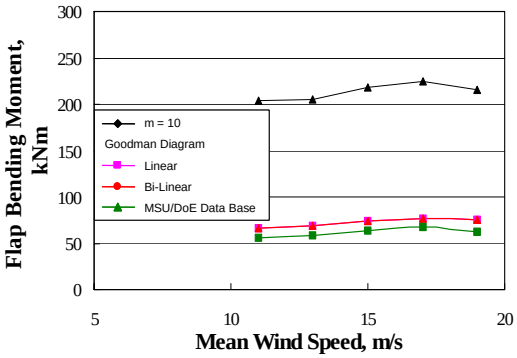

Fig. 9b: Flapwise Bending Moment

Fig. 8: Equivalent Fatigue Loads for the LIST Turbine on the Tensile Bending Side

Fig. 9: Equivalent Fatigue Loads for the ART on the Tensile Bending Side

The comparison of the four formulations in Figs. 8 and 9 indicates that there is a major difference between the power law model and Goodman diagrams. In particular, the power law model predicts a significantly higher EFL at all values of wind speeds for both turbines. For the Bushland turbine, the linear and bi-linear Goodman diagrams (Figs. 2a and 2b, respectively) predict similar EFL, while the full diagram (Fig. 2c) predicts a relatively small decrease in the EFL from the other two Goodman diagrams for three of the four load spectra. For the fourth spectra (Fig. 8b), the MSU/DoE model predicts similar results. Similar results are shown for the ART data.

While the comparisons to the power law formulation cited here have some very important implications, the reader is cautioned against drawing a broad interpretation from these comparisons. In particular, the power law formulation is not dependent on the mean stress. Thus, the EFL at R = –1 (reverse tension and compression) and R = 0.1 (all tensile loads) are the same for this formulation. This result is not consistent with experimentally determined S-N curves for fiberglass composites because the failure mode for fiberglass is different in compression than it is in tension. Thus, the comparisons are almost like comparing "apples to oranges." To minimize any discrepancies, all of the comparisons presented here are based an R-value of –1 and to the ultimate compressive strength. Comparisons to other R-values will have different results.

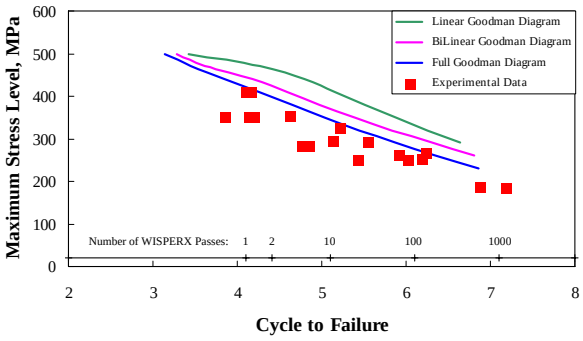

Fig. 10a: Failures Predicted Using the Mean Goodman Diagram

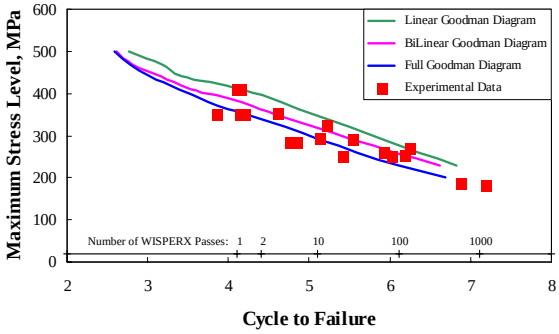

Fig. 10b: Failures Predicted Using the 95/95 Goodman Diagram

Fig. 10: Comparison of Experimental Data to Predicted Failure using Linear Miner's Rule

WISPERX Load Spectra

The experimental cycles-to-failure as a function of the maximum stress in the spectrum for material DD16 are shown in Fig. 10 [10]. In these figures, Miner's rule [1] was used to predict failure of the coupon specimens subjected to WISPERX spectrum using the mean-value and the 95/95 Goodman diagrams (see Figs. 2 and 3). The linear Goodman diagram predicts the longest lifetimes (cycles-to-failure) and the full Goodman diagram predicts the shortest lifetimes. Notice that the mean-Goodman-diagram fits do not pass through the mean of the data: rather, all three formulations predict service lifetimes that are significantly higher than the measured lifetime. The comparison of the predictions using the 95/95 Goodman diagram illustrates that they also predicted service lifetimes that are higher than the measured lifetime, with the full 95/95 Goodman diagram predicting lifetimes near the mean of the experimental data.

Thus, Miner's rule does not predict the measured lifetimes very well. And, even the 95/95 Goodman diagrams are non-conservative in that they predict longer service lifetimes than those measured in the tests using the WISPERX load spectrum. At best, the full 95/95 Goodman diagram predicts the mean of measured data. Although not discussed here, non-linear residual strength rules do offer better predictions of the failure data [8,12].

Concluding Remarks

The effect of mean stress on the prediction of damage from typical wind turbine load spectra is analyzed using a detailed Goodman diagram. This detailed formulation of the S-N behavior of fiberglass composites is obtained by constructing a Goodman diagram using S-N curves at thirteen different R-values. The data used in this process is contained in the MSU/DoE Fatigue Database for composite materials. This diagram is the most detailed to date, and it includes several loading conditions that have been poorly represented in earlier studies.

The analysis illustrates the effect of the detailed Goodman diagram relative to other formulations of the S-N behavior of the fiberglass composite. The results of the comparison using experimentally-measured fatigue loads illustrates that a power law formulation is the most

conservative; namely, it produces the highest EFL. When compared to one another, the linear and bi-linear formulations yield essentially the same damage estimates, with the bi-linear formulation being slightly less conservative than the linear. Depending on the nature of the load spectrum, both the linear and the bi-linear formulations are conservative when compared to the detailed MSU/DoE formulation.

The results of the analysis of the WISPERX experiments illustrate that when a Miner's rule damage criterion is used, the mean fits of the data do not predict failure very well, while the 95/95 predicts failures near the mean of measured data.

Thus, the MSU/DoE formulation of the Goodman diagram with a detailed representation of thirteen R-values indicates that the effects of mean stress are more important than previously thought. The region where the composite is transitioning between compressive and tensile failure modes in particularly important and the updated Goodman diagram provides a better description of this region.

REFERENCES

1. Sutherland, H.J., *On the Fatigue Analysis of Wind Turbines*, Report SAND99-089, Sandia National Laboratories, Albuquerque, NM (1998)

2. Mandell, J.F., and D.D. Samborsky, *DOE/MSU Composite Material Fatigue Database: Test Methods, Materials, and Analysis*, Report SAND97-3002, Sandia National Laboratories, Albuquerque, NM (1997).

3. Mandell, J.F., D.D. Samborsky, and D.S. Cairns, *Fatigue of Composite Materials and Substructures for Wind Turbine Blade*" Contractor Report SAND2002-077, Sandia National Laboratories, Albuquerque, NM, 2002.

4. Mayer, R.M., *Design of Composite Structures Against Fatigue*, Mechanical Engineering Publications Ltd., Suffolk, G.B. (1996).

5. van Delft, D.R.V., G.D. de Winkel and P.A. Joosse, "Fatigue Behavior of Fiberglass Wind Turbine Blade Material Under Variable Amplitude Loading," *1997 ASME Wind Energy Symposium*, AIAA/ASME, pp. 180-188.

6. Nijssen, R.P.L, D.R.V. van Delft and A.M. van Wingerde, "Alternative Fatigue Lifetime Prediction Formulations for variable Amplitude Loading," *2002 ASME Wind Energy Symposium*, AIAA/ASME, pp. 10-18

7. Mandell, J.F., D.D. Samborsky, N.K. Wahl, and H. J. Sutherland, "Testing and Analysis of Low Cost Composite Materials Under Spectrum Loading and High Cycle Fatigue Condition," Conference Paper, *ICCM14*, Paper # 1811, SME/ASC, 2003, 10 p.

8. Sutherland, H.J., and J.F. Mandell, "The Effect of Mean Stress on Damage Predictions for Spectral Loading of Fiberglass Composite Coupons," *Specialty Conference on Making Torque from the Wind*, EWEC, 2004, in publication.

9. Sutherland, H.J., and J.F. Mandell, "Effect of Mean Stress on the Damage of Wind Turbine Blades," *2004 ASME Wind Energy Symposium*, AIAA/ASME, 2004.

10. Ten Have, A.A., *WISPER and WISPERX: Final Definition of Two Standardized Fatigue Loading Sequences for Wind Turbine Blades*, NLR-TP-91476U, National Aerospace Laboratory NLR, Amsterdam, the Netherlands, 1992.

11. Mandell, J.F., D.D. Samborsky, D.W. Combs, M.E. Scott and D.S. Cairns, *Fatigue of Composite Material Beam Elements Representative of Wind Turbine Blade Substructure*, Report NREL/SR-500-24374, National Renewable Energy Laboratory, Golden, Co, 1998.

12. Wahl, N.K., J.F. Mandell, D.D. Samborsky, S*pectrum Fatigue Lifetime and Residual Strength for Fiberglass Laminates*, Report SAND2002-0546, Sandia National Laboratories, Albuquerque, NM, 2002.

13. Kensche, C.W., "Effects of Environment," *Design of Composite Structures Against Fatigue*, R. M. Mayer, ed., Mechanical Engineering Pub. Limited, Bury St Edmunds, Suffolk, UK, 1996, pp.65-87

15. Sutherland, H.J., P.L. Jones, and B. Neal, 2001, "The Long-Term Inflow and Structural Test Program," *2001 ASME Wind Energy Symposium*, AIAA/ASME, pp. 162-172.

16. Sutherland, H.J., "Analysis of the Structural and Inflow Data from the LIST Turbine," *Journal of Solar Energy Engineering*, Transactions of the ASME, v. 124, November, 2002, pp. 432-445.

17. Sutherland, H.J., J.R. Zayas, A.J. Sterns and B. Neal, 2004, "Update of the Long-Term Inflow and Structural Test Program," *2001 ASME Wind Energy Symposium*, AIAA/ASME, in publication.

18. Kelley, N., M. Hand, S. Larwood, and E. McKenna, 2002, "The NREL Large-Scale Turbine Inflow and Response Experiment – Preliminary Results," *2002 ASME Wind Energy Symposium*, AIAA/ASME, pp. 412-426.

19. Sutherland, H.J., N.D. Kelley and M.M. Hand, "Inflow and Fatigue Response of the NWTC Advanced Research Turbine," *2003 ASME Wind Energy Symposium*, AIAA/ASME, 2003, pp. 214-224.